Biomimetic Dendrimer–Peptide Conjugates for Early Multi-Target Therapy of Alzheimer's Disease by Inflammatory Microenvironment Modulation

Peixin Liu, Tongyu Zhang, Qinjun Chen, Chao Li, Yongchao Chu, Qin Guo, Yiwen Zhang, Wenxi Zhou, Hongyi Chen, Zheng Zhou, Yu Wang, Zhenhao Zhao, Yifan Luo, Xuwen Li, Haolin Song, Boyu Su, Chufeng Li, Tao Sun, and Chen Jiang*

Current therapeutic strategies for Alzheimer's disease (AD) treatments mainly focus on β-amyloid (Aβ) targeting. However, such therapeutic strategies have limited clinical outcomes due to the chronic and irreversible impairment of the nervous system in the late stage of AD. Recently, inflammatory responses, manifested in oxidative stress and glial cell activation, have been reported as hallmarks in the early stages of AD. Based on the crosstalk between inflammatory response and brain cells, a reactive oxygen species (ROS)-responsive dendrimer–peptide conjugate (APBP) is devised to target the AD microenvironment and inhibit inflammatory responses at an early stage. With the modification of the targeting peptide, this nanoconjugate can efficiently deliver peptides to the infected regions and restore the antioxidant ability of neurons by activating the nuclear factor (erythroid-derived 2)-like 2 signaling pathway. Moreover, this multi-target strategy exhibits a synergistic function of ROS scavenging, promoting Aβ phagocytosis, and normalizing the glial cell phenotype. As a result, the nanoconjugate can reduce ROS level, decrease Aβ burden, alleviate glial cell activation, and eventually enhance cognitive functions in APPswe/PSEN1dE9 model mice. These results indicate that APBP can be a promising candidate for the multi-target treatment of AD.

1. Introduction

Alzheimer's disease (AD) is a progressive neurodegenerative disease with complex pathogenesis.[1] The current clinical or preclinical drugs for treating AD include single-target drugs. In recent years, there has been significant interest concerning excessive production and aggregation of amyloid-β (Aβ).[2] However, the pay is not proportional to the return, as numerous clinical trials were successively terminated.[3] An increasing number of studies have revealed that therapeutic strategies focused on targeting Aβ can be insufficient.[4] Therefore, it is important to seek new pathogeny and more therapeutic targets to modulate the AD microenvironment.

The overall features of the microenvironment and intricate crosstalk among cells in the brain have recently been considered as hallmarks of AD.[5] The early AD microenvironment is characterized by inflammatory responses and oxidative stress, which were reported to precede the appearance of the amyloid cascade.[6] Inflammation is often accompanied by immune system activation, which is ultimately mediated primarily by glial cells, such as microglia and astrocytes.[7] Among all non-neuronal CNS cells, microglia are the most intimately associated with tissue changes that are observed in AD. Microglia are believed to control the balance of metabolism in the brain, including the secretion of proinflammatory or anti-inflammatory cytokines and phagocytosis of abnormal proteins. However, under the AD circumstance, the balance is interrupted and excessive toxic agents can contribute to abnormal AD microenvironment, which in turn causes damage to neurons, worsens inflammatory responses, and accelerates AD progression.[8] Recent studies have indicated that targeting microglia may result in more beneficial therapeutic outcomes. For example, interferon-γ enhanced glycolysis of microglia and restored the migration and phagocytosis ability to clear Aβ burden, which further rescued cognitive memory of 5XFAD transgenic mice.[9] Further, activating triggering the receptor expressed on myeloid cells 2-apolipoprotein E signaling pathway of microglia restored the homeostatic signature and prevented the neuronal loss in an acute model of neurodegeneration.[10] These results are regarded as favorable evidence for consideration of microglia as the core of modulation in the early stage of AD, providing a new perspective for treatment.

In addition, oxidative stress has been shown in a wide range of studies to contribute significantly to the pathogenesis and

P. Liu, T. Zhang, Q. Chen, C. Li, Y. Chu, Q. Guo, Y. Zhang, W. Zhou,
H. Chen, Z. Zhou, Y. Wang, Z. Zhao, Y. Luo, X. Li, H. Song, B. Su, C. Li,
Prof. T. Sun, Prof. C. Jiang
Key Laboratory of Smart Drug Delivery
Ministry of Education
State Key Laboratory of Medical Neurobiology and MOE Frontiers Center
for Brain Science
Department of Pharmaceutics
School of Pharmacy
Fudan University
Shanghai 201203, P. R. China
E-mail: jiangchen@shmu.edu.cn

The ORCID identification number(s) for the author(s) of this article
can be found under https://doi.org/10.1002/adma.202100746.

**ADVANCED
SCIENCE NEWS**

www.advancedsciencenews.com

**ADVANCED
MATERIALS**

www.advmat.de

progression of AD in the early stage.[11] Prolonged or excessive microglial cell activation may produce cytokines, chemokines, ROS, and nitric oxide, which sustain the oxidative microenvironment. ROS is a typical characteristic of oxidative stress and an important initiator of neuronal damage. Correcting the abnormal microenvironment of the lesion by eliminating the oxidative stress cascade reaction has been proven as a new perspective with significant great potential for early AD treatment. For example, our group previously reported that phenylboronic-based micelles encapsulating curcumin regulated the microglial inflammatory microenvironment;[12] ceria-based (CeO₂) nanozymes switched the phenotype of microglia by catalyzing the decomposition reaction of excess ROS.[13] In addition, accumulating evidence has pointed out that it is important to reactivate the cellular antioxidant capacity to defend ROS in the oxidative microenvironment.[14] Although scavenging excessive ROS is confirmed as an effective means for normalizing oxidative stress, modulating the function of damaged cells from a further upstream perspective is a new therapeutic strategy that has significant potential for long-term treatment of AD.

Nuclear factor (erythroid-derived 2)-like 2 (Nrf2) plays a central role in cellular redox homeostasis.[15] It was mainly maintained at a relatively low protein level in the cytoplasm by Kelch-like ECH-associated protein 1 (Keap1), which was labeled as the resting state under normal conditions. Under the stimulation of external oxidative stress, Nrf2 is activated and translocated into the nucleus. This process initiates the transcription of downstream antioxidant proteins that protect cells from oxidative damage. However, Nrf2 mainly exists in the cytoplasm of hippocampal neurons, and the nuclear protein level is significantly decreased in the AD microenvironment.[16] Deficiency of the Nrf2-mediated signaling pathway can cause accumulation of ROS and damage to neurons. Moreover, numerous studies have shown that the deletion of Nrf2 is closely associated with microglial activation and Aβ generation.[17] Therefore, Nrf2 is the key component that controls the antioxidant system and modulates the AD microenvironment. Activation of the Nrf2-mediated signaling pathway might have the potential for AD treatment.

Peptide-based therapeutics are agents that exhibit significant efficacy for inhibition of protein-protein interactions. Moreover, compared with small molecules that are utilized in the treatment of AD, such as curcumin and resveratrol, most therapeutic peptides have specific targets of signaling pathways that have been well demonstrated in vitro and in vivo. The peptide LQLDEETGEFLPIQ (designated p-Nrf2), which is based on the Nrf2 binding region to the Kelch domain of Keap1 was reported to competitively bind to Keap1 and promote Nrf2 to enter the nucleus.[18] However, peptides generally exhibit disadvantages resulting from their small size and high polarity upon systemic administration, which may lead to poor pharmacokinetics and bioavailability.[19] Polymer-drug conjugate (PDC) is a classic delivery strategy in the nanomedicine field because of its high stability in circulation and its applicable size (10–100 nm) for targeting and penetration, which has been widely investigated.[20] Traditional PDCs are usually composed of mono drug molecules and long linear polymers; hence, they have a low drug loading content. Dendrimer–peptide conjugates (DPCs) have received significant attention as a novel class of PDCs

with high drug loading content, easy modification, and good stability.[21]

However, the existence of the blood–brain barrier (BBB) limits the transportation of most therapeutic peptides or biomacromolecules. Although therapeutic agents can be delivered into the brain with the help of delivery systems, the AD locus selectivity was unsatisfactory. It was reported that Aβ could be easily internalized into the brain. The internalization can be mediated by the highly expressed receptor for advanced glycation end-products (RAGE), which is closely related to the progression of AD.[22] Inspired by the transportation of Aβ, KLVFFAED (designated Ab peptide), derived from Aβ without interfering with normal signal transduction, was reported to be capable of actively targeting the AD lesion area via RAGE.[23] Hence, utilization of Ab peptide-modified LDPDC is a promising strategy for therapeutic peptides delivery for AD treatment.

Herein, we report a peptide delivery system (APBP) inspired by DPC with the ability to target the AD microenvironment and inhibit the inflammatory response (**Scheme 1**). The nanoconjugate is composed of three components: an Ab peptide, a poly (ethylene glycol) (PEG)-based phenylboronic dendrimer (PB) with ROS responsiveness and clearing ability, and a therapeutic peptide, p-Nrf2. The nanoconjugate could effectively span the BBB and bind to RAGE, which is highly expressed in the AD microenvironment. By eliminating ROS and releasing p-Nrf2, it had a synergistic effect of restoring cellular antioxidant capacity and alleviating glial cell activation. Inhibition of inflammatory responses and neuroprotective effects in the early stages of AD has been demonstrated in vitro and in vivo. Moreover, the present study demonstrates that multi-target therapy can enhance the therapeutic effects compared with a single target in the early stage of AD, and might have a better potential for clinical translation.

2. Results and Discussion

2.1. Preparation and Characterization of APBP Nanoconjugates

The phenylboronic containing dendrimer of nanoconjugates was synthesized via linking 8-arm hydroxylating PEG and ROS-sensitive alkynyl linker with 4-nitrophenyl chloroformate (Figure S1, Supporting Information). In brief, 8-arm hydroxylating PEG was obtained from MeO-PEG-NH₂ (M_w = 5000) or N₃-PEG-NH₂ (M_w = 5000) through three rounds of acylation and acid hydrolysis. The synthesized 8-arm hydroxylating PEG was first activated with 4-nitrophenyl chloroformate in a previous study and then conjugated with alkynyl phenylboronic ester via nucleophilic attack reaction.[24] The chemical composition of the polymer was verified by ¹H NMR (Figures S2–S13, Supporting Information). To achieve the brain and AD microenvironment accumulation, a RAGE-targeting peptide KLVFFAED (designated Ab peptide) was applied. The C terminal of the peptide was modified with alkynyl group and linked with 8-arm hydroxylating PEG by copper(I)-catalyzed click reaction. Similarly, LQLDEETGEFLPIQ (designated p-Nrf2), which can activate the Nrf2 mediating antioxidant signaling pathway was modified with the azide group of the C terminal and linked with

**ADVANCED
SCIENCE NEWS**

www.advancedsciencenews.com

**ADVANCED
MATERIALS**

www.advmat.de
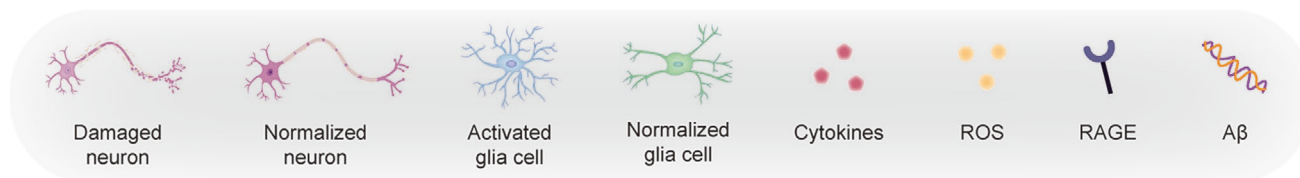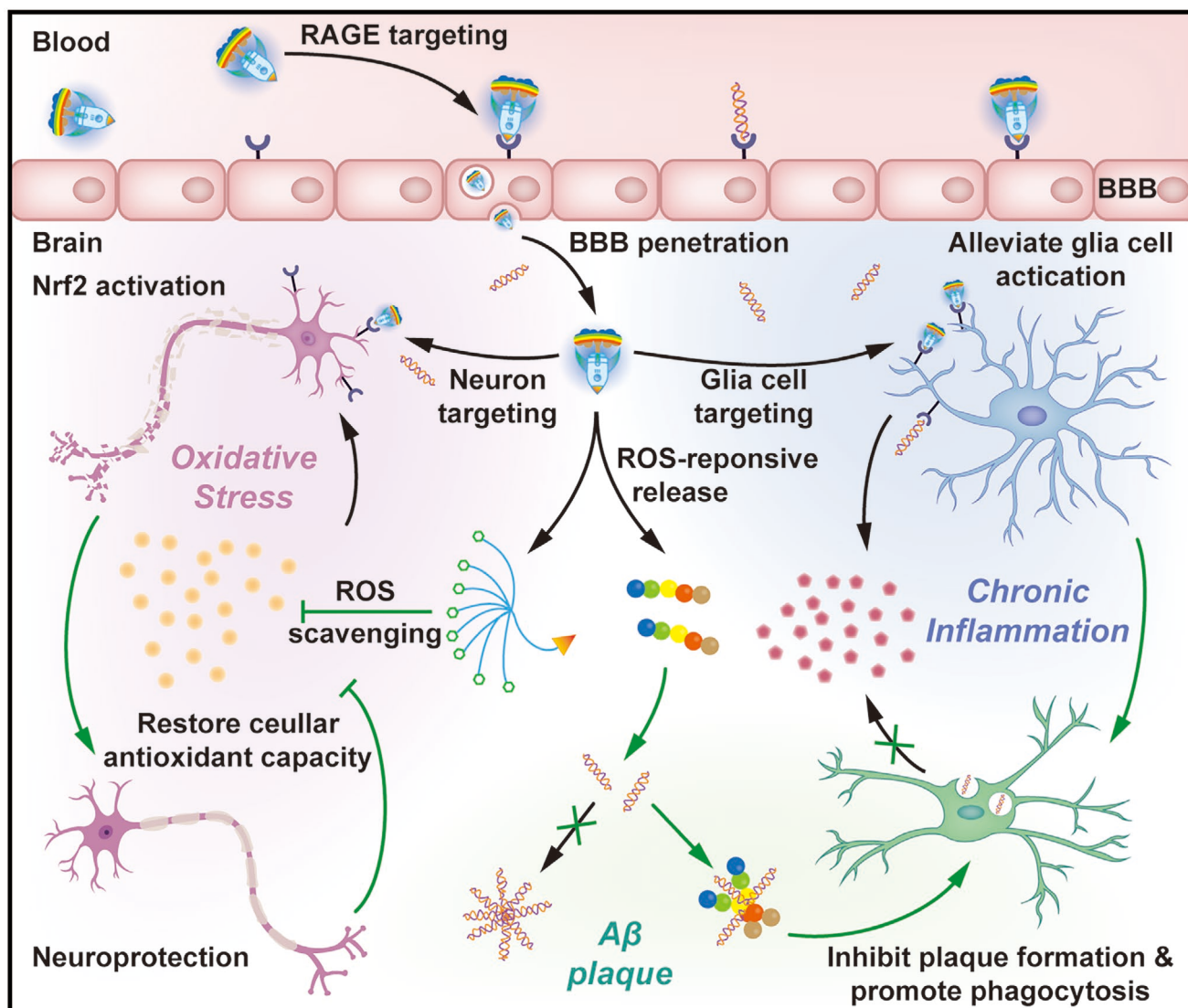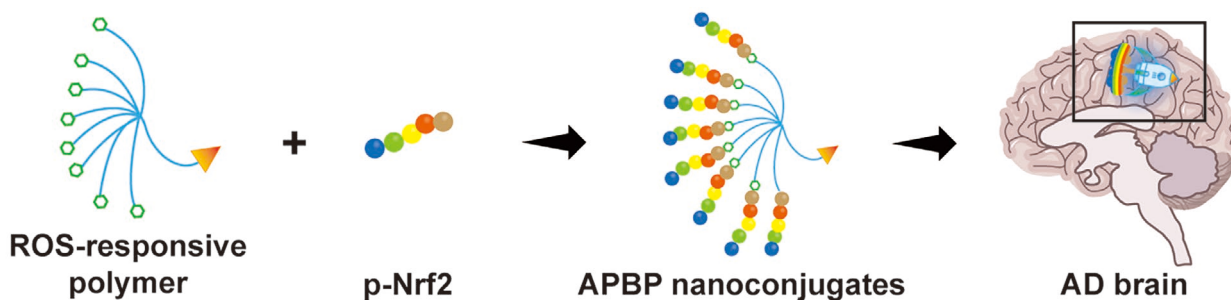
Scheme 1. Illustration of APBP nanoconjugate formation and AD microenvironment modulation: 1) brain parenchyma accumulation and damaged cells uptake via RAGE targeting; 2) ROS-responsive release of ROS scavenging polymer and Nrf2 signaling pathway activating p-Nrf2; and 3) multitarget therapy is achieved by restoring cellular antioxidant capacity, alleviating glial cell activation, and promoting Aβ phagocytosis.
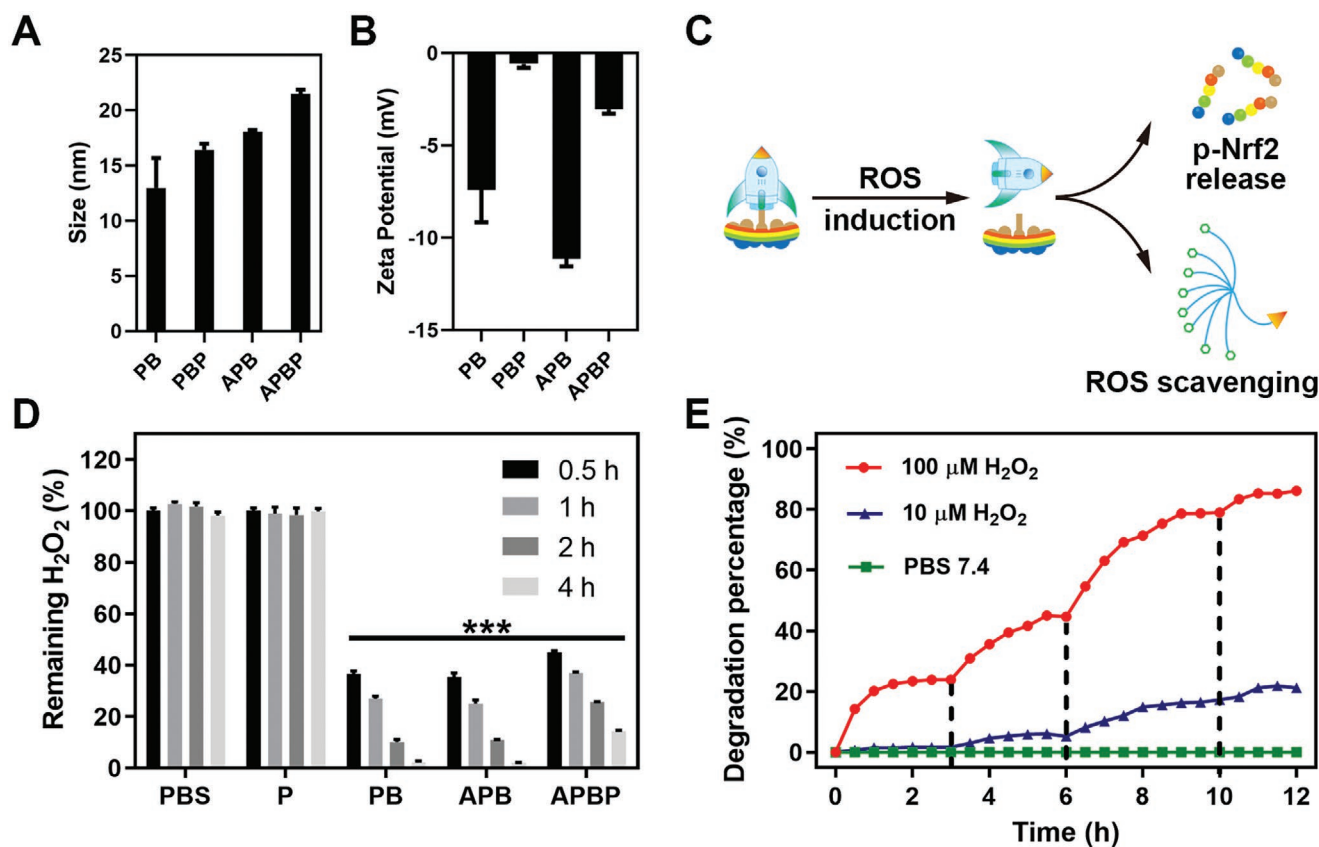
Figure 1. Characteristics and ROS responsiveness of formulations. A) Size distribution of representative formulations measured by DLS. B) Zeta potential of representative formulations. C) The mechanism of ROS induced self-immolative degradation to release peptide. D) ROS scavenging ability of formulations. E) The kinetics of polymer degradation release under PBS 7.4 or pulsed H_2O_2 (1×10^{-4} or 1×10^{-5} M). The arrows indicate extra added H_2O_2 stimulation after H_2O_2 went out. Results are reported as means ± SD (n = 3, ***$P < 0.001$).

an 8-arm hydroxylating PEG by the same reaction. Successful synthesis and conjugation of representative products were demonstrated by decreased elution time in gel-permeation chromatography result (Figure S16, Supporting Information). Three kinds of nanoconjugates were prepared: Ab peptide modified or unmodified nanoconjugates with p-Nrf2 linked (designated APBP or PBP respectively) and Ab peptide modified nanoconjugates with scramble peptide linked (designated APBS, Figure S15, Supporting Information). Dynamic light scattering (DLS) results showed that the hydrodynamic diameter of an 8-arm hydroxylating PEG was around 13 nm and increased to around 16 nm with p-Nrf2 modification. Linking of Ab peptide to PBP elevated the size to about 18 nm and the diameter of final nanoconjugate (APBP) was around 21 nm (**Figure 1**A). Zeta potential of nanoconjugates was generally negatively charged which could avoid the absorbance of protein in the circulation after systemic administration (Figure 1B). Ab peptide modification could slightly decrease the zeta potential of nanoconjugates, while the zeta potential value was significantly increased due to the conjugate of p-Nrf2. The drug-loading of nanoconjugates was measured by ^1H NMR after purification (Figure S14, Supporting Information). To be specific, the peak in the spectrum found between ≈1.0–0.5 ppm indicated hydrogen of methyl in the compound. While, each p-Nrf2 molecule contains eight methyl, which indicated that around 4.8 p-Nrf2, molecules were

conjugated to the polymers. Drug loading was calculated as around 50%. Due to the favorable size, appropriate zeta potential, and high drug loading, the nanoconjugates could serve as a novel platform for peptide brain-targeting delivery.

Next, we evaluated the ROS scavenging and sensitive release abilities of nanoconjugates to demonstrate their antioxidant ability. The mechanism of ROS scavenging and sensitive release was illustrated in Figure 1C. Briefly, the self-immolative electronic elimination process of phenylboronic ester could be induced when exposed to H_2O_2 (Figure S17, Supporting Information).[25] This process would cause the elimination of ROS and sensitive release of p-Nrf2. First, 100×10^{-6} M H_2O_2 was incubated with p-Nrf2 or nanoconjugates for specific time schedules. Then the remaining concentration of H_2O_2 was measured immediately. Polymers (PB), blank nanoconjugates (APB), and p-Nrf2 linked conjugates (APBP) exhibited great potential concerning ROS elimination (Figure 1D) due to the presence of phenylboronic ester group in the structure. Contrarily, the free p-Nrf2 (P) group scarcely showed any changes in H_2O_2 concentration. Especially, H_2O_2 concentrations decreased by around 60% after a 2-h incubation with PB, APB, and APBP, and almost cleared after a 4-h incubation. This result exhibited the fast ROS scavenging ability of nanoconjugates, which could meet the demand of inhibiting the progression of the inflammatory microenvironment in the early stage of AD. The results

**ADVANCED
SCIENCE NEWS**

www.advancedsciencenews.com

**ADVANCED
MATERIALS**

www.advmat.de

suggested that these nanoconjugates could serve as a good agent to sweep ROS and protect neurons.

The kinetics of nanoconjugate degradation was further investigated to explore the sensitive release behavior of p-Nrf2. Nanoconjugates were incubated in PBS 7.4, with or without 1×10^{-4} M H_2O_2 in vitro, to stimulate the inflammatory and normal microenvironment.[26] 4-Hydroxybenzylalcohol, a degradation marker, was detected by high-performance liquid chromatography (HPLC) every 30 min to monitor the degradation speed of the nanoconjugates in H_2O_2 (Figure S18, Supporting Information). As shown in Figure 1E, the nanoconjugates exhibited a unique release pattern of pulsatile degradation. Due to the fast ROS scavenging ability of the nanoconjugates, the release pattern tended to be stable with the decrease in H_2O_2 concentration, however, the release was quickly restored with the addition of H_2O_2. In comparison, approximately 20% degradation was observed in the 1×10^{-5} M H_2O_2 concentration treatment group, and no degradation was observed in nanoconjugates incubated with only PBS 7.4, which also demonstrated the specific release behavior of nanoconjugates. In addition, the degradation product detected by ^{1}H NMR (Figure S19, Supporting Information) was the benzene peak of 4-hydroxybenzylalcohol found between 7.5 and 6.5 ppm.

2.2. Investigation on Cellular Uptake and Transportation Across the BBB In Vitro

Ab peptide (KLVFFAED) has been reported as a binding peptide with RAGE derived from $A\beta$, which is nontoxic and an ideal agent for brain targeting.[27] The stability of the Ab peptide in the ROS environment was first verified with MOLDI-TOF, which demonstrated the targeting stability of APBP in the AD microenvironment (Figure S20, Supporting Information). To evaluate the efficiency of nanoconjugate targeting, SH-SY5Y cells, BV2 cells, and brain capillary endothelial cells (BCECs) were used as in vitro models for neurons, microglia, and the BBB, as they were all reported to express RAGE (Figures S21 and S24, Supporting Information).[28] Hek293T cells were used as the negative control, which showed hardly any RAGE expression (Figure S21, Supporting Information). FITC-labeled PBP and APBP were prepared to characterize cellular uptake. Significantly increased fluorescence signals were observed in both APBP-treated SH-SY5Y and BCECs cells compared with the PBP group (Figure S22, Supporting Information), indicating that Ab peptide modification could significantly enhance the cellular uptake due to the expression of RAGE. To further investigate the mechanisms of nanoconjugate internalization, different inhibitive uptake conditions were treated with SH-SY5Y and BCECs cells, including filipin for caveolin inhibition, wortmannin for macropinocytosis inhibition, chlorpromazine for clathrin inhibition, and 4 °C for energy inhibition. As illustrated in **Figure 2**A, the uptake was inhibited by chlorpromazine at 4 °C, indicating an energy-and clathrin-dependent pathway. In addition, the fluorescence decreased significantly with free Ab peptide pre-treatment. This result demonstrated the dominant role of the Ab peptide in the internalization process. Meanwhile, the uptake behavior of APBP-FITC in BECE cells showed a caveolin-and macropinocytosis-dependent

pathway (Figure S23, Supporting Information). Noticeably, the inhibitive effect of Ab peptide on SH-SY5Y cells was found stronger than that on BCECs. This phenomenon may attribute to the different mechanisms of transportation and expressed levels of RAGE on cells.[29] The upregulated uptake of APBP in $A\beta_{1-42}$-activated microglia was further investigated in a BV2 cell model. As shown in Figure 2B and Figure S24A, Supporting Information, APBP was largely internalized by $A\beta_{1-42}$-activated BV2 cells compared to untreated BV2 cells. Interestingly, enhanced uptake was not observed in $A\beta_{1-42}$-activated BV2 cells treated with PBP. This phenomenon could be attributed to the upregulated expression of RAGE in $A\beta_{1-42}$-activated BV2 cells (Figure S24B, Supporting Information).

Moreover, we proved that APBP could span the BBB via RAGE in vitro with a BCECs monolayer transwell system (Figure 2C). BCECs cells were allowed to grow for around 11 days on a gelatin-coated insert to meet the resistance value of 200 Ω cm^2 (Figure S25A, Supporting Information).[30] The fluorescence of the reception pool was measured to evaluate their permeability across BCECs monolayer transwell system. As a result, APBP showed greater transport ability compared with PBP and this process could be inhibited by pre-incubation with free Ab peptide revealing the RAGE-mediated transport (Figure 2D). No significant changes concerning integrity and stability were observed before, during, and after the treatment (Figure 2E; Figure S25B, Supporting Information). In addition, the ^{14}C-sucrose permeability value of different groups was below the standard value of primary cell monolayer, which could also guarantee the integrity of this system (Figure 2F; Figure S25C, Supporting Information). According to the above results, we suggested that Ab peptide-modified nanoconjugates could efficiently cross the BBB in vitro.

2.3. Evaluation of Brain-Targeting Ability and Intracerebral Distribution

RAGE is reported to be highly expressed in AD lesions, which enhances $A\beta$ transportation and worsens inflammatory responses.[31] Six-month-old APP/PS1 mice were used to evaluate the distribution of APBP and PBP, as RAGE was highly expressed in the lesions compared with wild type (WT) mice.[32] Thus, APBP and PBP were labeled with a hydrophobic near-infrared probe boron-dipyrromethene (BODIPY) to track their fate in vivo. Further, they were injected intravenously into APP/PS1 and WT mice. A strong brain fluorescence signal was observed in APBP/BODIPY-treated mice and isolated tissues at 4 h post-administration compared with PBP/BODIPY-treated mice (Figure 2G; Figure S26, Supporting Information). Moreover, the quantitative analysis of radiant efficiency and injection dose percentage (ID %) showed that APBP/BODIPY was highly accumulated in the brain compared with PBP/BODIPY-treated mice (Figure 2H,I). It is worth noting that the ID% of APBP/BODIPY-treated APP/PS1 mice was significantly higher than that of APBP/BODIPY-treated WT mice, indicating high expression of RAGE-mediated transportation in vivo. In addition, fluorescence imaging of frozen brain sections was performed to analyze the pathway of the nanoconjugates. As shown in Figure 2J, additional red signals of the probe were observed in
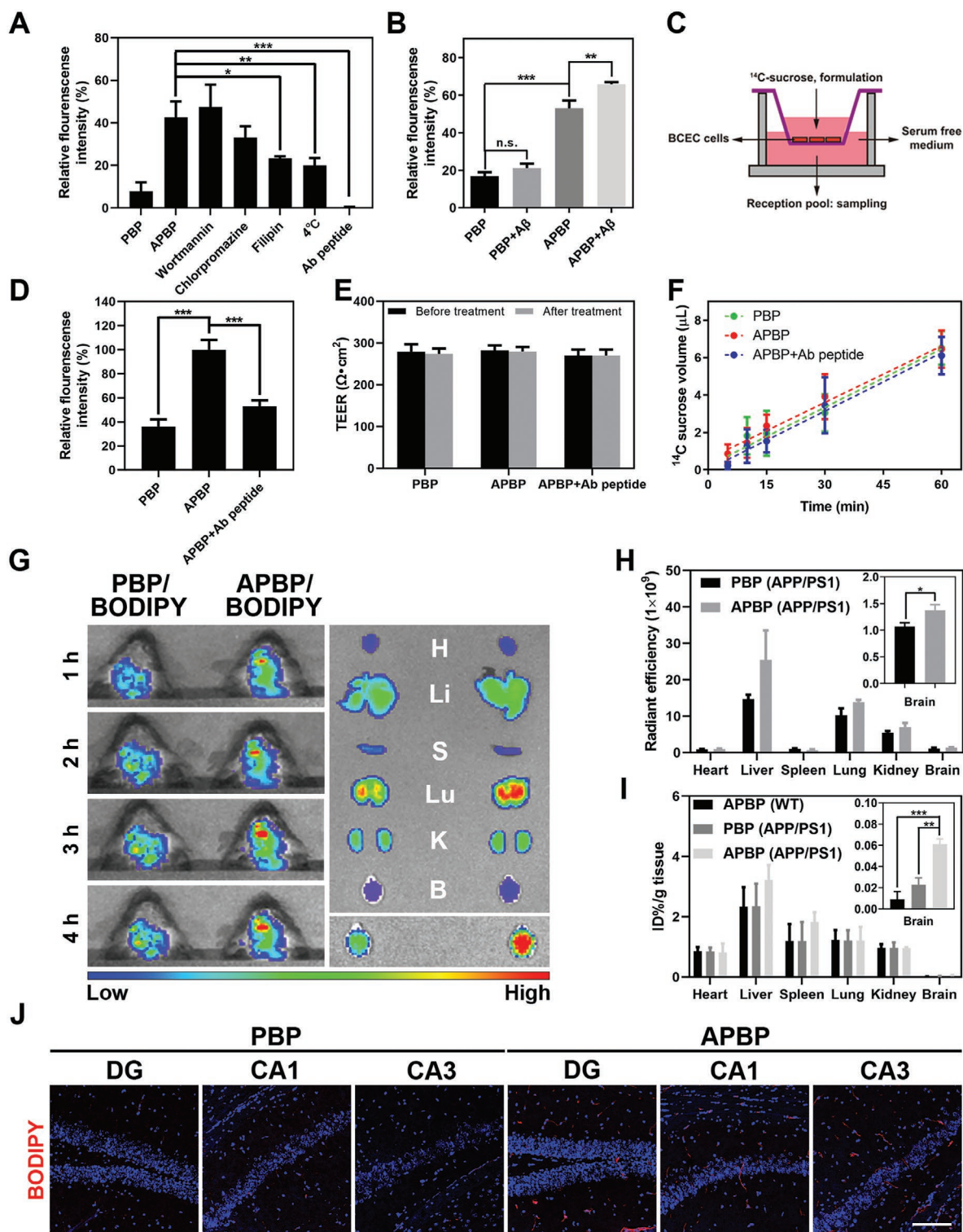
Figure 2. Distribution and fate of APBP in vitro and in vivo. A) Cellular uptake in SH-SY5Y cells under different inhibitive conditions. B) Cellular uptake in Aβ-activated BV2 microglia cells. C) Illustration of the BCECs monolayer transwell system to simulate the BBB in vitro. D) Relative fluorescence intensity under the reception pool of different treatment groups at 1 h. E) TEER measurement before and after the experiment. F) ^{14}C-sucrose permeability during the experiment. G) In vivo imaging of APP/PS1 mice administrated with PBP-BODIPY with or without Ab peptide modification. Images were taken 4 h after intravenous administration. Organs were labeled with the initial character (H for heart, Li for liver, S for spleen, Lu for lung, K for kidney, and B for brain). H) Radiant efficiency of BODIPY fluorescence intensity in major organs and brain. I) ID% analysis of BODIPY accumulation in major organs and brain. J) Fluorescence imaging of major AD lesion areas in APP/PS1 mice after ex vivo in vivo imaging system (IVIS) imaging (red: BODIPY; blue: 4′,6-diamidino-2-phenylindole (DAPI)). Scale bar: 100 μm. Results are reported as means ± SD (n = 3, *P < 0.05, **P < 0.01, or ***P < 0.001).

**ADVANCED
SCIENCE NEWS**

www.advancedsciencenews.com

**ADVANCED
MATERIALS**

www.advmat.de

the DG, CA1, and CA3 regions in the hippocampus treated with APBP/BODIPY compared with unmodified nanoconjugates, indicating selective targeting of AD lesion areas.

In summary, Ab peptide modification could facilitate BBB penetration of nanoconjugates and subsequent selective accumulation in AD disease areas. Based on this, nanoconjugates could be actively internalized by damaged neurons and active glial cells and then responsively release p-Nrf2 to modulate AD microenvironment.

2.4. Nanoconjugate-Mediated Restoration of Cellular Antioxidant Capacity and Neuroprotection In Vitro

Previous studies have reported that neurons are sensitive to oxidative stress and can easily undergo caspase-dependent apoptosis.[33] To evaluate the antioxidative and neuroprotective ability of nanoconjugates, H_2O_2 or aggregated $A\beta_{1-42}$ was applied to induce apoptosis in SH-SY5Y cells, which is in line with the damage of neurons observed in AD patients.[34] First, the cellular toxicity of p-Nrf2 and polymers was evaluated by CCK-8 assay. The results indicated that significant cell death was not observed with incubation with SH-SY5Y cells and BCECs (Figures S27 and S28, Supporting Information). Then, the ROS level was detected using the ROS probe H2DCFDA in the $A\beta_{1-42}$-treated cell model (**Figure 3**A; Figure S29, Supporting Information). The green ROS signal notably decreased after APBP treatment and was close to that of the control group. Interestingly, the ROS level of the APBP group was even lower than that of the APBS group, which contained the same molar weight of phenylboronic ester. This result indicates that the antioxidant capacity of damaged cells was restored by p-Nrf2. To further verify the neuroprotective effect of the nanoconjugates, Annexin V-fluorescein (FITC)/propidium iodide (PI) double staining assay of $A\beta_{1-42}$-treated cell model (Figure 3B; Figure S30, Supporting Information) and CCK-8 assay of H_2O_2 induced apoptosis model (Figure 3C) were performed. The tests revealed similar results, which revealed that the anti-apoptotic effect of APBP was better than that of APBS.

A combination of the above results revealed that phenylboronic ester-based nanoconjugates exhibited favorable anti-oxidative stress ability while APBP showed greater ROS scavenging ability and neuroprotective effect with p-Nrf2 modification than scramble peptide modified APBS. This phenomenon may be attributed to p-Nrf2 mediated cellular antioxidant capacity activation. Nrf2 signaling pathway is usually inhibited by Keap1 in the cytoplasm and can be translocated into the nucleus to stimulate the expression of antioxidant proteins.[35] This process is a natural program that occurs in cells to fight against oxidative stress. Unfortunately, the Nrf2 signaling pathway is impaired in AD affected brain regions, thus it fails to protect cells from damage.[36] To illustrate the mechanisms of neuroprotection, we further investigated the level of activated Nrf2 in the nucleus of SH-SY5Y cells upon being treated with nanoconjugates in the $A\beta_{1-42}$-treated cell model. As shown in Figure 3D, increased expression of Nrf2 was observed in the nucleus after APBP treatment, while Nrf2 signal was rarely observed in the nucleus in the $A\beta_{1-42}$-treated group due to the activation dysfunction. Expression levels of nucleus Nrf2 and downstream antioxidant

protein were further explored to substantiate whether the impaired Nrf2 signaling pathway was restored and cellular antioxidant capacity was recovered. Similar results were obtained that indicated that APBP could promote the transportation of Nrf2 into the nucleus and expression of downstream antioxidant proteins, including GCLM, HO-1, and NQO1 (Figure 3E). Moreover, scramble peptide group APBS also exhibited the effect of activating Nrf2 signaling pathway, which might be attributed to the ROS scavenging ability, thus relieving the damage to the cells' natural function. Taken together, the above assay demonstrated that APBP nanoconjugates could eliminate ROS in the microenvironment and restore cellular antioxidant capacity via phenylboronic ester mediated self-immolative reaction and activation of Nrf2 dependent antioxidant signaling pathway (Figure 3F).

2.5. In Vitro Modulation of Microglia Activation and Immunologic Function

Microglia, the sentinels of inflammation and injury in the central nervous system, maintain homeostasis of normal tissues. However, microglia are extremely sensitive to infection and can become activated or dysregulated, which may contribute to disease severity.[37] In the process of excessive activation, microglia adopt an "amoeboid" activated phenotype, which usually refers to an inflammatory M1-like phenotype.[38] Polarization of M1-type microglia to an anti-inflammatory M2-like phenotype was reported to have significant potential for normalizing the brain microenvironment.[39] To investigate whether the phenotype of the $A\beta_{1-42}$-activated BV2 cell line was altered after treatment with APBP, the expression of M1 (CD16/32) and M2 (CD206) markers was comprehensively evaluated in vitro. As shown in **Figure 4**A, Figures S31 and S32, Supporting Information, co-incubation of $A\beta_{1-42}$ could cause the elevation of the M1 marker in BV2 cells, which demonstrated the proinflammatory state of microglia in the AD microenvironment. Interestingly, p-Nrf2 treatment reduced the level of CD16/32, while a significant increase was observed in CD206. In addition, CD206 levels increased after treatment with APBS, while the CD16/32 levels did not change compared with the $A\beta_{1-42}$ treatment. This phenomenon revealed that p-Nrf2 could mainly modulate proinflammatory microglia by activating the Nrf2 signaling pathway, while scavenging ROS with phenylboronic ester helped increase the anti-inflammatory phenotype (Figure S33, Supporting Information). These effects could be further strengthened with the combination of p-Nrf2 and phenylboronic ester-based polymers, since a decrease in M1 marker and an increase in M2 marker were observed upon APBP treatment (Figure S26, Supporting Information). In addition, similar results were found for the expression of proinflammatory cytokines (tumor necrosis factor-α, TNF-α and interleukin 6, IL-6) and anti-inflammatory cytokines (interleukin 10, IL-10 and arginase, Arg1) in BV2 cells activated by $A\beta_{1-42}$ (Figure 4B,C). It was reported that scavenging ROS could initiate the M2-like polarization of microglia, while the decreased M1-like phenotype was not obvious, which was also observed in the group treated with APBS.[40] Activation of the Nrf2 mediated signaling pathway with p-Nrf2 delivery was found to reduce the level of
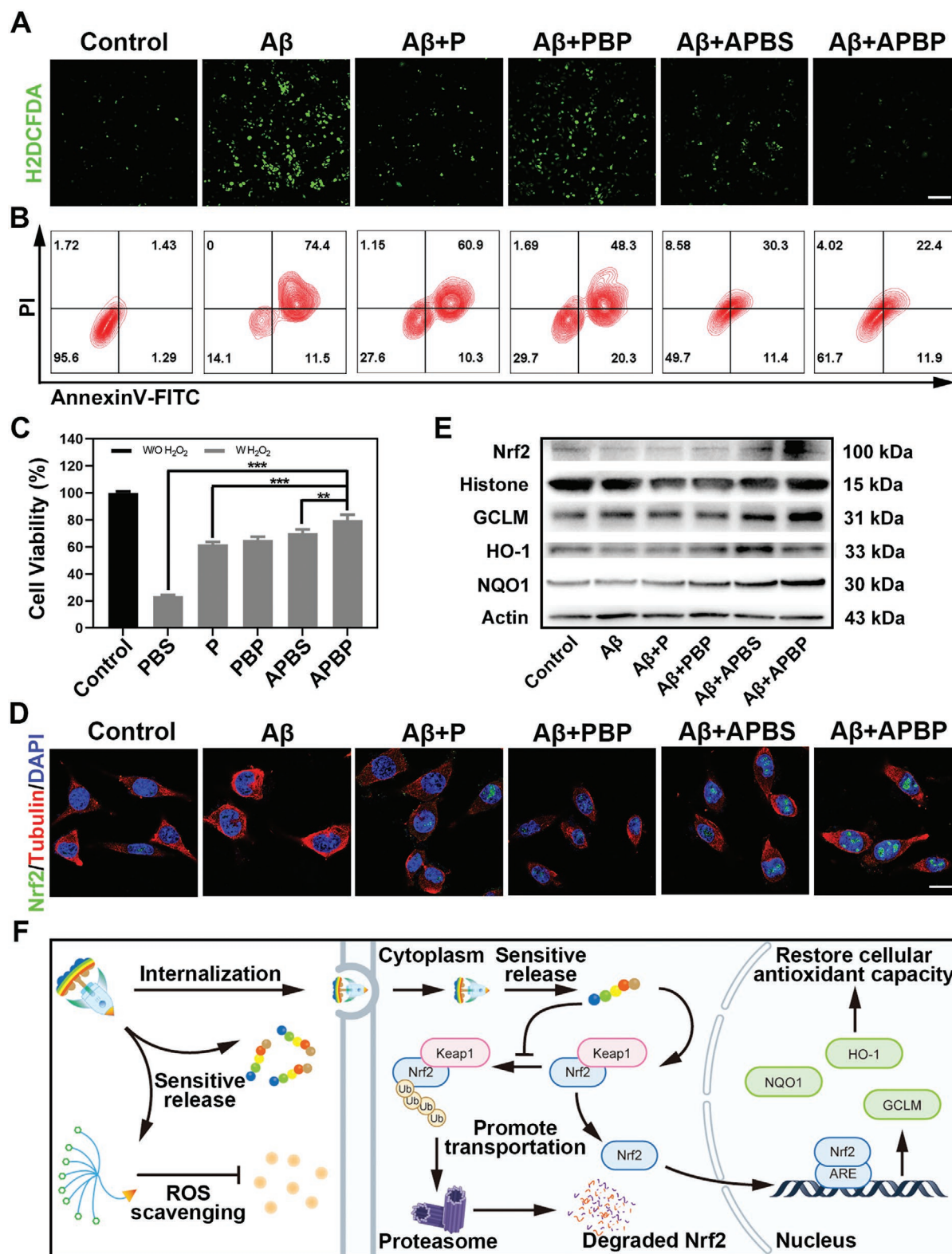
Figure 3. Neuroprotection of APBP via ROS scavenging and Nrf2 induction. A) Cellular oxidative stress in the presence of $A\beta_{1-42}$ (green: oxidized H2DCFDA fluorescence). Scale bar: 50 µm. B) Flow cytometry analysis images of cell apoptosis gating on Annexin V-FITC/PI staining. C) Cell viability of SH-SY5Y cells treated with different formulations in the presence of H_2O_2. D) Confocal images of nucleus Nrf2 expression in SH-SY5Y cells treated with $A\beta_{1-42}$ (blue: DAPI for nucleus, red: α-Tubulin for cell cytoskeleton, green: Nrf2). Scale bar: 20 µm. Results are reported as means ± SD (n = 3, *$P < 0.05$, **$P < 0.01$, or ***$P < 0.001$). E) Western blotting of Nrf2 signaling pathway-associated protein expression in SH-SY5Y cells treated with different conditions. F) Scheme of the mechanisms of neuroprotection.
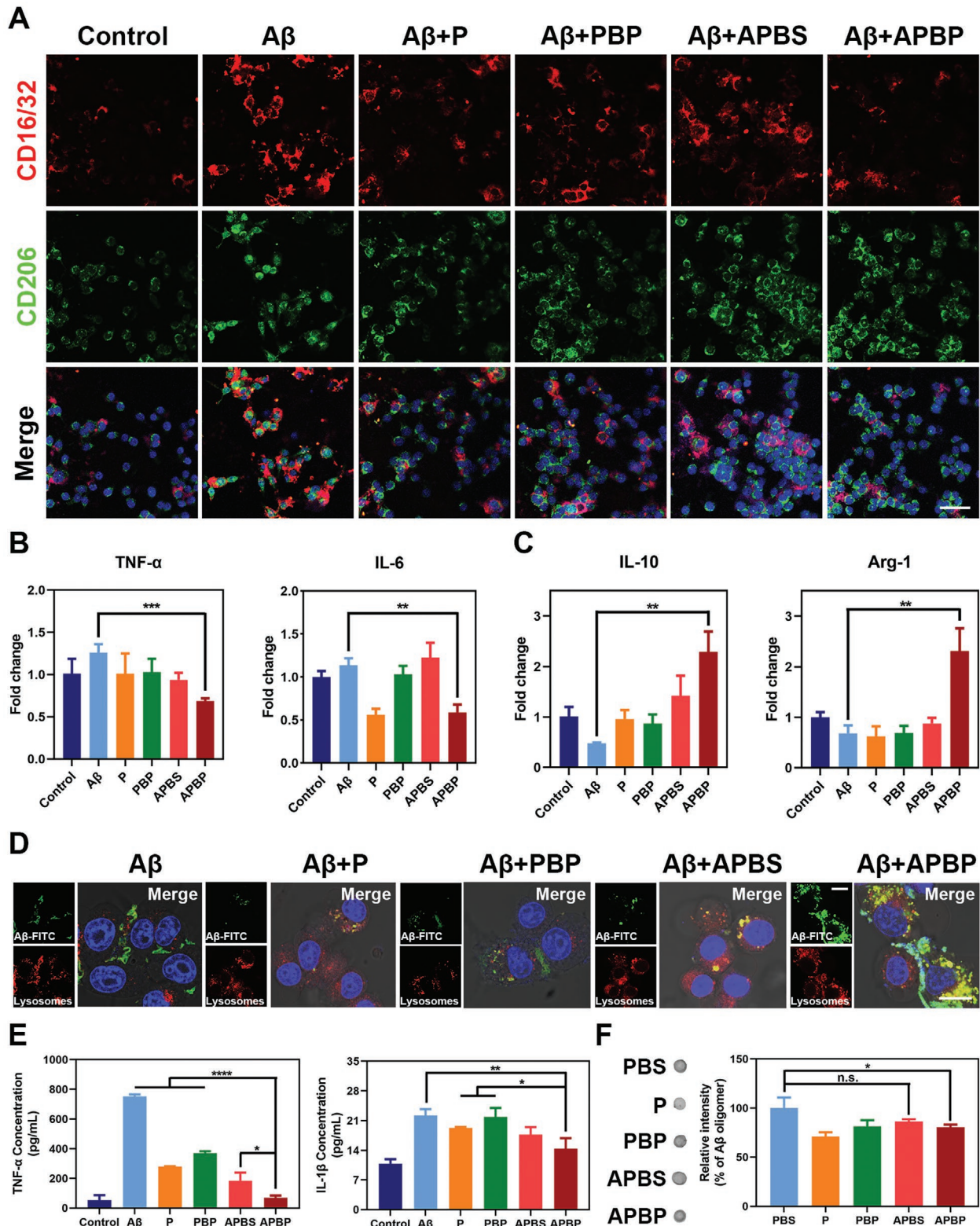
Figure 4. Modulation of microglia inhibitive and inflammatory microenvironment in vitro. A) Immunostaining of CD16/32 (M1 marker) and CD206 (M2 marker) of BV2 cells. Cells were treated with Aβ_{1-42} along with different formulations for 24 h. Scale bar: 50 μm. B) mRNA relative expression of M1 phenotype markers TNF-α and IL-6 of BV2 cells. C) mRNA relative expression of M2 phenotype markers IL-10 and Arg1 of BV2 cells. D) Confocal images of FITC labeled Aβ_{1-42} distributed in BV-2 cells at 4 h. Scale bar: 20 μm. E) Levels of TNF-α and IL-1β in the supernatants of BV2 cells treated with different formulations were determined by using ELISA kits. F) Dot blot image of Aβ_{1-42} after incubation with different formulations and quantitative results. Results are reported as means ± SD (n = 3, *$P < 0.05$, **$P < 0.01$, ***$P < 0.001$, or ****$P < 0.0001$).

M1 type microglia. Furthermore, this phenotype modulation effect was also demonstrated in a ROS-stimulated cell model (Figure S34, Supporting Information). Thus, the combination of activating the Nrf2 signaling pathway and ROS scavenging might become a promising microglial phenotype polarization strategy for AD treatment.

As the immune cells in the CNS, microglia play a central role in Aβ clearance. Aβ could be degraded through lysosomal/autophagy or proteasomal pathway.[41] However, the phagocytosis function of microglia is dysregulated due to excessive activation and the inflammatory microenvironment.[42] Restoration of the immunologic function of microglia in the early stage of AD shows great potential concerning the alleviation of Aβ-mediated neurotoxicity. To examine the effect of nanoconjugates on microglia-mediated Aβ clearance, confocal laser scanning microscopy (CLSM) and flow cytometry were performed. As shown in Figure 4D, Aβ-FITC-treated BV2 cells exhibited little green signal inside cells and green fluorescence was primarily observed on the cell membrane which is in accord with previous reports.[43] After co-incubation with APBS, the yellow fluorescence signal showed that Aβ was internalized into the cells and colocalized with lysosomes, suggesting that relieving oxidative stress could facilitate the clearance of Aβ. This effect could be enhanced by APBP treatment due to the restoring of cellular antioxidant capacity by p-Nrf2. Flow cytometry data also supported the above results (Figure S35, Supporting Information). Moreover, the colocalization of green Aβ-FITC fluorescence and red lysosome fluorescence further confirmed that APBP facilitated Aβ clearance through lysosomal network of microglia.

It has been reported that Aβ can trigger the secretion of pro-inflammatory cytokines such as TNF-α and IL-1β.[44] The excessive accumulation of these cytokines in the microenvironment might cause damage to microglial immunologic function and, in turn, worsen AD progression. Thus, we evaluated the effect of nanoconjugates on the attenuation of Aβ-induced inflammation. As displayed in Figure 4E, the supernatant level of TNF-α increased to approximately 750 pg mL^{-1} for Aβ_{1-42} incubated alone. Treatment with APBP significantly reduced the secretion of TNF-α, which was consistent with the control group. Furthermore, APBP also noticeably controlled the upregulation of IL-1β, and this effect was more pronounced compared with the other groups. According to the amyloid theory, soluble Aβ monomers can aggregate into oligomer type during AD progression, which is the most toxic form of causing inflammatory responses.[45] To further investigate the mechanisms underlying the effects of APBP on Aβ clearance and alleviation of Aβ-induced inflammation. A dot blot assay was performed to evaluate the interaction between the nanoconjugates and the Aβ_{1-42} monomer. As shown in Figure 4F and Figure S36, Supporting Information, aggregation of the Aβ_{1-42} monomer was strongly inhibited by P and APBP, while a significant inhibitory effect was not observed in the APBS group. This result demonstrated that p-Nrf2 could disturb the Aβ aggregation process and thus alleviate neurotoxicity and glial cell activation. DLS results showed smaller Aβ aggregation after treatment with P, PBP, and APBP, while the size of Aβ aggregation was more than 1 µm in the PBS and APBS groups (Figure S37, Supporting Information). Molecular docking simulation was also

performed to further explain the interaction between p-Nrf2 and the Aβ_{1-42} monomer/oligomer (Figure S38, Supporting Information). The results demonstrated that p-Nrf2 could interact with the Aβ_{1-42} monomer/oligomer binding domain, which contributed to the inhibition of Aβ aggregation and promotion of Aβ clearance.

The combination of ROS scavenging and inhibition of Aβ aggregation could protect microglia from external stimulation, which further promoted the normalization of phenotype polarization and immunological function. This multi-target strategy alleviated inflammatory responses caused by activated microglia.

2.6. Nanoconjugates Rescue the Memory Decline of AD Model Model Mice

APP/PS1 transgenic mice were used to investigate the effect of nanoconjugates concerning the restoration of cellular antioxidant capacity and alleviation of glial cell activation in vivo. The treatment schedule is shown in **Figure 5**A. Briefly, the therapy was administered after the targeting ability of nanoconjugates was verified at the age of 6 months. This stage of mice demonstrated early symptoms of AD in this model.[46] Saline, p-Nrf2, and nanoconjugates were administered via tail vein weekly for 3 months, and pathological monitoring and therapeutic evaluation were performed after each month. After three months of treatment, memory and cognitive improvement were tested using the Morris Waster maze and nesting behavior. After 6 days of training, AD mice treated with APBP exhibited remarkably shorter escape latencies than those in the saline-treated group, whereas limited improvement was observed in mice treated with P, PBP, and APBS (Figure 5B,C). In addition, the APBP group spent more time in the targeted quadrant and crossed the hidden platform more times than the other groups. As the hippocampus is mainly involved in AD pathology, nesting experiments were performed to evaluate the function of this brain area after treatment.[47] As shown in Figure 5D,E, and Figure S39, Supporting Information, AD mice could not build a complete and mass nest due to the cognitive decline deficiency, while the nest score was improved after treatment with APBP, which was almost comparable to that of WT mice. These results demonstrated that APBP treatment significantly attenuated cognitive and memory impairments in AD transgenic mice.

2.7. Oxidative Stress Modulation and Underlying Mechanisms In Vivo

Although AD aetiology and pathogenesis were not fully understood, oxidative stress is considered a key component. Oxidative stress has been shown in a wide range of studies to contribute significantly to the pathogenesis and progression of AD.[48] Accumulation of an excessive amount of ROS in AD microenvironment would cause damage to neurons and activate microglia.[49] Thus, in order to understand the ROS scavenging ability and neuroprotective effect of nanoconjugates, the level of ROS and neuronal viability was monitored during the treatment.
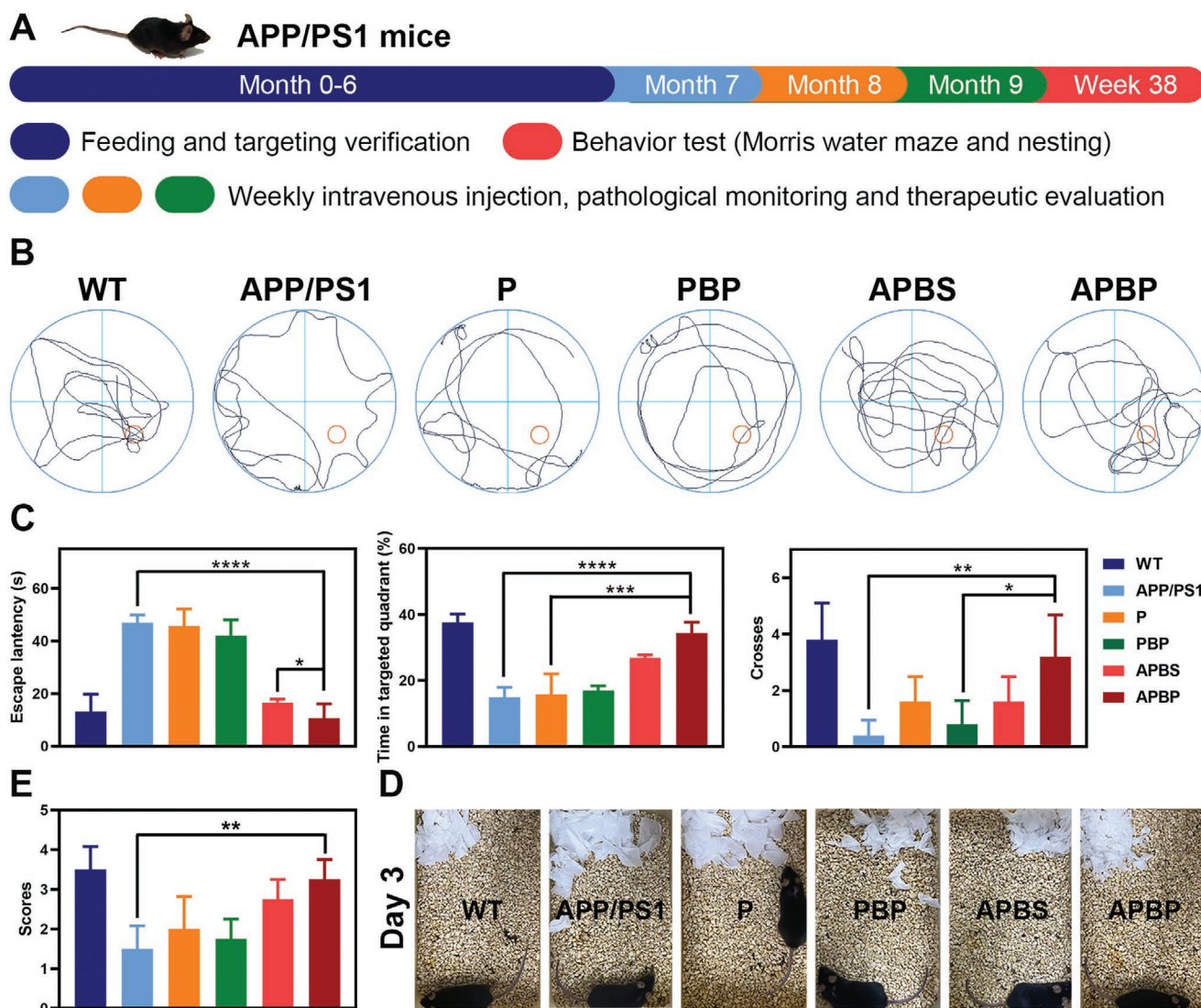
Figure 5. APBP improved learning skills and memory of APP/PS1 mice. A) Time schedule of drug treatment, pathological monitoring, and therapeutic evaluation. B) Representative swimming paths of mice in Morris water maze. C) Escape latency, swimming time spent in the targeted quadrant and crosses over the platform site. D) Representative images and E) quantitative analysis of nest behavior was obtained in the APP/PS1 mice and compared to the age-matched WT mice on day three. Results are reported as means ± SD (n = 3, *$P < 0.05$, **$P < 0.01$, ***$P < 0.001$, or ****$P < 0.0001$).

First, 8-hydroxyguanosine (8-OHG), an oxidative damage product, was utilized to determine the level of ROS in the brain.[50] A significant increase in the green fluorescence signal of 8-OHG was observed in the hippocampus and cortex of APP/PS1 9-month old mice compared to APP/PS1 6-month old mice, which was consistent with results obtained in the clinical trials (Figures S32 and S33, Supporting Information).[51] Surprisingly, alleviation of oxidative stress was observed in the first month (M7) of APBP treatment (**Figure 6**A; Figures S40, S41, and S42, Supporting Information). In addition, this effect was sustained until the third month of therapy. We assumed that the nanoconjugate could quickly respond to the high level of ROS in the AD microenvironment and eliminate excessive ROS via the degradation of phenylboronic-ester-based polymers. Notably, the level of ROS was slightly elevated after treatment with APBS for 3 months. This phenomenon could demonstrate that it was not

enough to sweep the ROS in the microenvironment, and activation of the antioxidant capacity of cells was more important for long-term treatment. Although the level of oxidative stress was relieved after treatment, the survival of neurons in the hippocampus should be considered. Next, we investigated whether the damaged neurons could be rescued by the nanoconjugates. NeuN, a neuronal marker, was found to display the density of neurons in the hippocampus. As shown in Figure 6B, Figures S43, S44, and S45, Supporting Information, obvious damage of neurons appeared in 9-month-old AD mice whose red fluorescence signals were significantly decreased compared with WT mice. After three months of treatment, the neuronal density of APBP-treated AD mice was noticeably enhanced and was similar to that of WT mice. Similar results were obtained by TUNEL staining (Figure S46, Supporting Information) and Nissl staining (Figure S47, Supporting Information). Moreover,
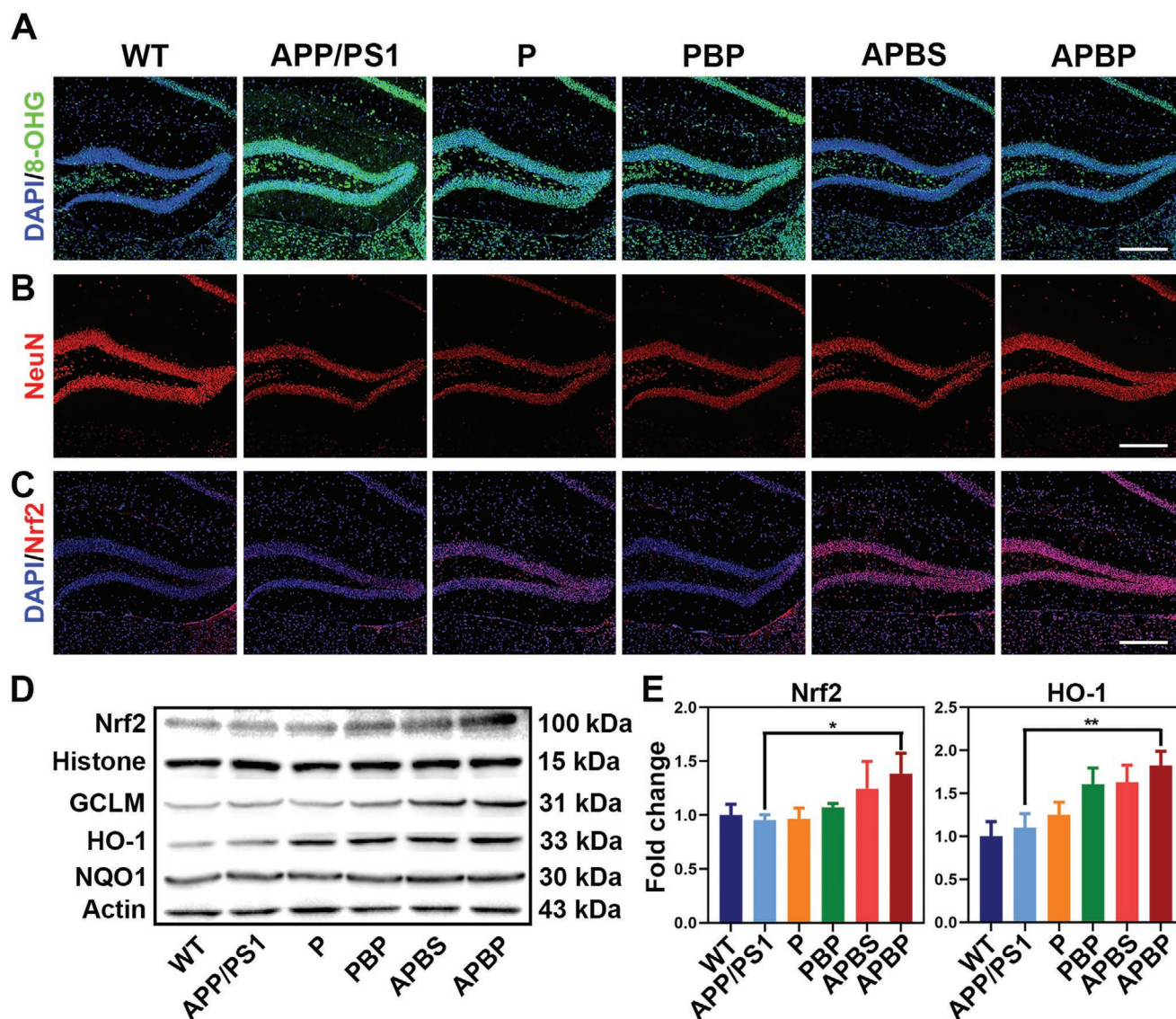
Figure 6. Mechanisms of APBP neuroprotection. A–C) Immunostaining of hippocampal, oxidative stress (green: 8-OHG), DG neurons (NeuN-positive cells, red), and Nrf2 expression (Nrf2, red). Scale bars: 100 μm. D,E) Western blotting of Nrf2 signaling pathway in brain after 3-month treatment and quantitative results. Results are reported as means ± SD (n = 3, *P < 0.05 or **P < 0.01).

the expression of RAGE was consistent with the progression of AD. The level of RAGE was found to decrease as the treatment progressed (Figures S48 and S49, Supporting Information), indicating the normalization of the brain microenvironment. Taken together, the oxidative stress level in the AD microenvironment could be controlled after APBP treatment and neuronal loss was inhibited from the early stage of AD.

To understand the mechanisms of APBP facilitated antioxidative stress and neuroprotection, we investigated the activation of the Nrf2-meidate signaling pathway in 9-month-old AD mice. As shown in Figure 6C and Figures S50 and S51, Supporting Information, Nrf2 of WT mice was kept in a resting state due to the resistance from Keap1. The red fluorescence of Nrf2 was still at a relatively low level under inflammatory stimulation and mainly located in the cytoplasm of cells. This

phenomenon demonstrated that the Nrf2-mediated signaling pathway was disabled in the AD microenvironment which could not protect neurons from oxidative damage. The expression of Nrf2 was enhanced slightly after treatment with APBS. Further, an increase in pink fluorescence signal was observed which showed that Nrf2 was translocated into the nucleus after activation. This result could indicate that ROS scavenging prevented the dysfunction of the Nrf2-mediated signaling pathway. Moreover, this effect could be further enhanced by APBP treatment due to the delivery of p-Nrf2, which could inhibit the interaction between Nrf2 and Keap1 and promote Nrf2 to enter the nucleus. It was reported that activation of Nrf2 could initiate the expression of antioxidant proteins including GCLM, HO-1, and NQO1.[52] Then, we further evaluated the protein level of Nrf2 and downstream antioxidant proteins in the

**ADVANCED
SCIENCE NEWS**
www.advancedsciencenews.com

**ADVANCED
MATERIALS**
www.advmat.de

hippocampus of AD mice brain. As shown in Figure 6D,E, and Figure S52, Supporting Information, expression of Nrf2 in the nucleus was similar to that observed in immunostaining experiments. Moreover, antioxidant proteins were all upregulated after treatment with APBP, which further confirmed the activation of Nrf2 and restoration of cellular antioxidant capacity. Thus, the above results indicated that nanoconjugates could not only efficiently scavenge ROS in the AD microenvironment but also restore cellular antioxidant capacity via activation of the Nrf2-mediated signaling pathway. We suggested that this joint strategy could maximize the effects of modulating oxidative stress in AD microenvironment.

2.8. Nanoconjugate-Alleviated Glia Cell Activation and Aβ-Induced Inflammation In Vivo

It has been reported that activation of glial cells and Aβ burden contribute to the formation of an inhibitory and inflammatory microenvironment in AD.[53] Encouraged by the results that nanoconjugates could polarize M1-like microglia to an M2-like phenotype and promote Aβ phagocytic activity of microglia in vitro, we wondered whether these effects could be achieved in APP/PS1 transgenic mice. After every month of treatment, the levels of activated microglia and Aβ plaques were monitored by immunostaining. As illustrated in Figures S53 and S54,
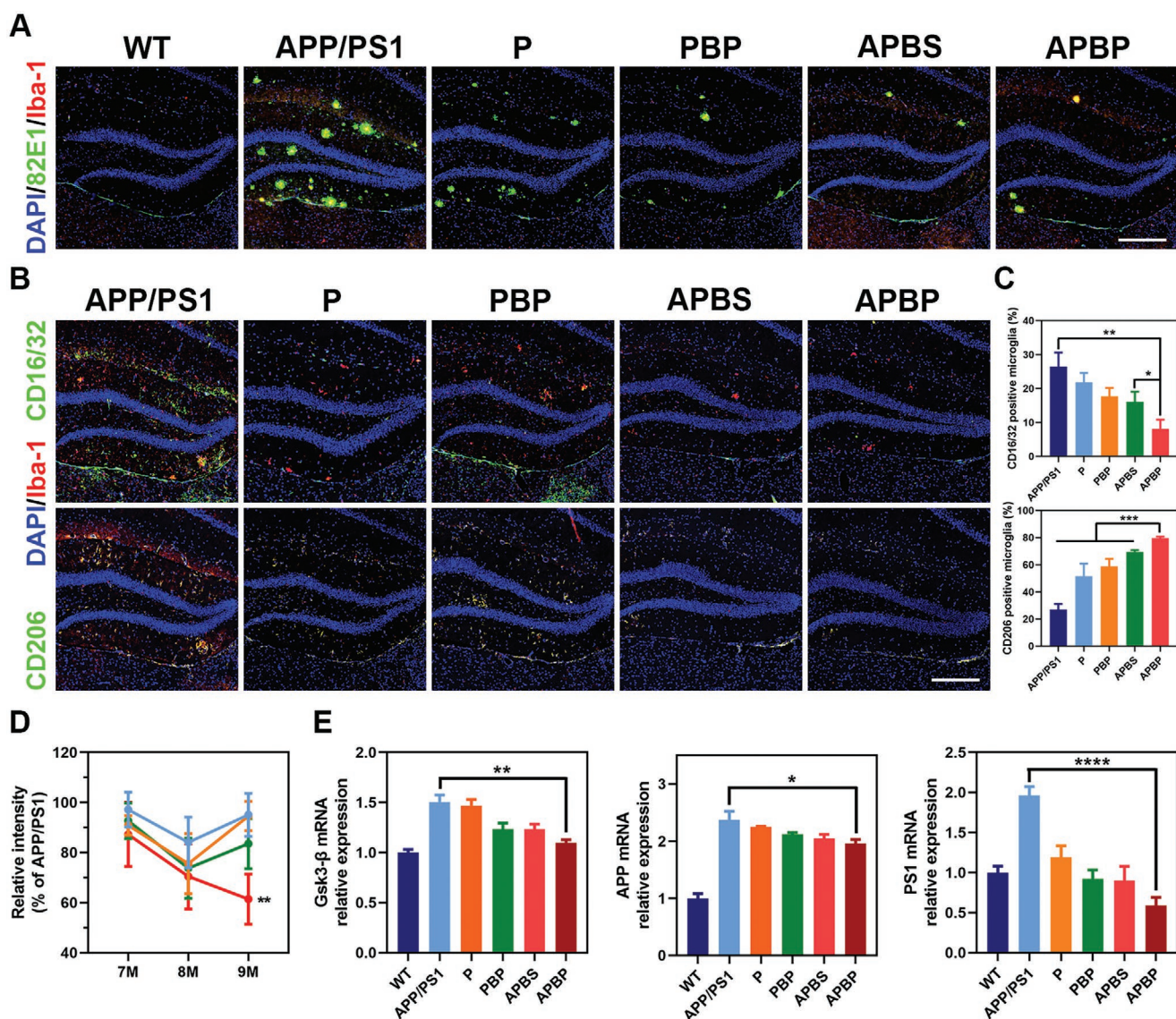

Figure 7. Mechanisms of APBP modulation of microglia and AD microenvironment. A) Immunostaining of neuroinflammation (Iba-1 for microglia, red; 82E1 for Aβ plaques, green; DAPI for nucleus, blue) in the hippocampus of mice treated with different formulations for two months(8M). Scale bar: 100 μm. B) Immunostaining of CD16/32 (M1 marker) and CD206 (M2 marker) (green: CD16/32 or CD206, red: Iba-1, blue: DAPI) to determine microglia phenotype in the hippocampus treated with different formulations. Scale bar: 100 μm. C) Quantification of CD16/32+ microglia and CD206+ microglia in hippocampus. D) Dot blot quantitative analysis of Aβ oligomer levels in the brains of WT and APP mice treated with different formulations. E) Relative expression of key proteins in the pathway of Aβ production in neurons. Results are reported as means ± SD (n = 3, *$P < 0.05$, **$P < 0.01$, ***$P < 0.001$, or ****$P < 0.0001$).

Supporting Information, massive microglial activation and Aβ burden were still observed in the hippocampus of AD mice after one-month (M7) treatment. Interestingly, these pathological indicators were significantly alleviated after two-month (M8) treatment and almost disappeared after the last month (M9) of treatment (**Figure 7**A). Similar effects on astrocytes were also observed after 3 months of treatment (Figures S55 and S56, Supporting Information). Noticeably, the relief of astrocyte activation occurred later than microglia, and this phenomenon could be explained by the quick response to the microenvironment changes of microglia, while astrocytes were mainly affected by activated microglia.[54] Next, the microglial phenotype was further examined after three months of treatment. As shown in Figure 7B,C, and Figures S57, S58, Supporting Information, the population of anti-inflammatory M2-type microglia increased in the brains of AD mice because of the increased expression of CD206+Iba-1+ cells as well as the reduced population of CD16/32+Iba-1+ cells. These effects were also substantiated by the decreased expression of the proinflammatory cytokines TNF-α and IL-1β (Figure S59, Supporting Information). As the normalized function of microglia in AD mice was achieved according to the above results, the protein level of Aβ plaques was further investigated. During treatment, a gradual decrease in Aβ oligomer levels was observed in mice treated with APBP nanoconjugates (Figure 7D and Figure S60, Supporting Information). In summary, APBP could modulate the AD microenvironment *by* alleviating glial cell activation and Aβ-induced inflammation.

To further understand the mechanisms of APBP facilitated microglia alleviation and normalized immunologic function, key proteins related to Aβ metabolism were investigated via examination of mRNA expression. GSK-3β mediated signaling pathway was reported to be highly expressed which was closely bound up with the increased Aβ burden in AD brains.[55] As shown in Figure 7E, the mRNA expression of glycogen synthase kinase-3β (GSK-3β), APP, and PS1 (γ-secretase) in the brain of APBP-treated mice were significantly inhibited. The activation of Nrf2 could in turn promote the inhibition of GSK-3β expression which was demonstrated in vitro previously.[56] Thus, we pointed out that APBP could modulate the inhibitory and inflammatory microenvironment via polarizing M1-type microglia to M2 phenotype and interrupt Aβ metabolism via inhibiting GSK-3β pathway. Additionally, negligible changes in the concentration of alanine transaminase (ALT) and aspartate transaminase (AST) suggested few liver toxicities caused by APBP after three months of treatment (Figure S61, Supporting Information). Furthermore, H&E staining results showed no pathological changes in the major organ sections excised from mice treated with multiple formulations, indicating the biosafety of the multi-target nanoconjugates (Figures S62 and S63, Supporting Information).

3. Conclusion

We have reported a multi-target and ROS-responsive peptide delivery nanoconjugate for modulating the AD microenvironment at an early stage. The levels of oxidative stress, Aβ plaques, and glial cell activation were all normalized by the synergistic effect of polymers and p-Nrf2, which further reversed the memory and cognitive decline in APP/PS1 mouse models. Compared with current nanoparticles focused on inflammatory responses in AD, our system not only scavenges ROS in the microenvironment, but also restores cellular antioxidant capacity by activating the Nrf2 signaling pathway to protect them. This strategy was devised with a focus on upstream target rather than only focusing on pathological abnormalities, which might have a better potential for clinical translation. Moreover, therapeutic effects that were more promising were achieved in vitro and in vivo when combined with re-educating activated glial cells and recovering their immunological function. Therefore, this multi-target nanoconjugate helps to explore the possibilities of rescuing AD progression at an early stage by focusing on normalizing cellular damage function and providing new perspectives concerning multi-target therapy for brain diseases.

Conflict of Interest

The authors declare no conflict of interest.

Data Availability Statement

Research data are not shared.

[1] a) F. Mangialasche, A. Solomon, B. Winblad, P. Mecocci, M. Kivipelto, *Lancet Neurol.* **2010**, *9*, 702; b) K. Yaffe, M. Tocco, R. C. Petersen, C. Sigler, L. C. Burns, C. Cornelius, A. S. Khachaturian, M. C. Irizarry, M. C. Carrillo, *Alzheimers Dement.* **2012**, *8*, 237.

**ADVANCED
SCIENCE NEWS**

www.advancedsciencenews.com

**ADVANCED
MATERIALS**

www.advmat.de

[2] a) C. L. Masters, R. Bateman, K. Blennow, C. C. Rowe, R. A. Sperling, J. L. Cummings, *Nat. Rev. Dis. Primers* **2015**, *1*, 15056; b) B. De Strooper, E. Karran, *Cell* **2016**, *164*, 603; c) H. Wang, X. Xu, Y. C. Pan, Y. Yan, X. Y. Hu, R. Chen, B. J. Ravoo, D. S. Guo, T. Zhang, *Adv. Mater.* **2020**, *33*, 2006483.

[3] a) T. M. Weitz, T. Town, *Immunity* **2016**, *45*, 717; b) D. R. Elmaleh, M. R. Farlow, P. S. Conti, R. G. Tompkins, L. Kundakovic, R. E. Tanzi, *J. Alzheimers Dis.* **2019**, *71*, 715.

[4] a) R. van der Kant, L. S. B. Goldstein, R. Ossenkoppele, *Nat. Rev. Neurosci.* **2020**, *21*, 21; b) M. Tolar, S. Abushakra, J. A. Hey, A. Porsteinsson, M. Sabbagh, *Alzheimers Res. Ther.* **2020**, *12*, 95; c) R. Loera-Valencia, A. Cedazo-Minguez, P. A. Kenigsberg, G. Page, A. I. Duarte, P. Giusti, M. Zusso, P. Robert, G. B. Frisoni, A. Cattaneo, M. Zille, J. Boltze, N. Cartier, L. Buee, G. Johansson, B. Winblad, *J. Intern. Med.* **2019**, *286*, 398.

[5] a) T. Bartels, S. De Schepper, S. Hong, *Science* **2020**, *370*, 66; b) J. C. Delpech, S. Herron, M. B. Botros, T. Ikezu, *Trends Neurosci.* **2019**, *42*, 361.

[6] a) F. L. Heppner, R. M. Ransohoff, B. Becher, *Nat. Rev. Neurosci.* **2015**, *16*, 358; b) D. A. Butterfield, B. Halliwell, *Nat. Rev. Neurosci.* **2019**, *20*, 148.

[7] S. Jevtic, A. S. Sengar, M. W. Salter, J. McLaurin, *Ageing Res. Rev.* **2017**, *40*, 84.

[8] H. Sarlus, M. T. Heneka, *J. Clin. Invest.* **2017**, *127*, 3240.

[9] S. H. Baik, S. Kang, W. Lee, H. Choi, S. Chung, J. I. Kim, I. Mook-Jung, *Cell Metab.* **2019**, *30*, 493.

[10] S. Krasemann, C. Madore, R. Cialic, C. Baufeld, N. Calcagno, R. El Fatimy, L. Beckers, E. O'Loughlin, Y. Xu, Z. Fanek, D. J. Greco, S. T. Smith, G. Tweet, Z. Humulock, T. Zrzavy, P. Conde-Sanroman, M. Gacias, Z. Weng, H. Chen, E. Tjon, F. Mazaheri, K. Hartmann, A. Madi, J. D. Ulrich, M. Glatzel, A. Worthmann, J. Heeren, B. Budnik, C. Lemere, T. Ikezu, F. L. Heppner, V. Litvak, D. M. Holtzman, H. Lassmann, H. L. Weiner, J. Ochando, C. Haass, O. Butovsky, *Immunity* **2017**, *47*, 566.

[11] a) C. Cheignon, M. Tomas, D. Bonnefont-Rousselot, P. Faller, C. Hureau, F. Collin, *Redox. Biol.* **2018**, *14*, 450; b) T. Jiang, Q. Sun, S. Chen, *Prog. Neurobiol.* **2016**, *147*, 1.

[12] Y. Lu, Z. Guo, Y. Zhang, C. Li, Y. Zhang, Q. Guo, Q. Chen, X. Chen, X. He, L. Liu, C. Ruan, T. Sun, B. Ji, W. Lu, C. Jiang, *Adv. Sci.* **2019**, *6*, 1801586.

[13] F. Zeng, Y. Wu, X. Li, X. Ge, Q. Guo, X. Lou, Z. Cao, B. Hu, N. J. Long, Y. Mao, C. Li, *Angew. Chem., Int. Ed.* **2018**, *57*, 5808.

[14] M. Zabel, A. Nackenoff, W. M. Kirsch, F. E. Harrison, G. Perry, M. Schrag, F. Radic, *Biol. Med.* **2018**, *115*, 351.

[15] Q. Ma, *Annu. Rev. Pharmacol. Toxicol.* **2013**, *53*, 401.

[16] a) P. Ren, J. Chen, B. Li, M. Zhang, B. Yang, X. Guo, Z. Chen, H. Cheng, P. Wang, S. Wang, N. Wang, G. Zhang, X. Wu, D. Ma, D. Guan, R. Zhao, *Oxid. Med. Cell. Longevity* **2020**, *2020*, 3050971; b) A. I. Rojo, M. Pajares, P. Rada, A. Nunez, A. J. Nevado-Holgado, R. Killik, F. Van Leuven, E. Ribe, S. Lovestone, M. Yamamoto, A. Cuadrado, *Redox Biol.* **2017**, *13*, 444.

[17] A. Osama, J. Zhang, J. Yao, X. Yao, J. Fang, *Ageing Res. Rev.* **2020**, *64*, 101206.

[18] S. C. Lo, X. Li, M. T. Henzl, L. J. Beamer, M. Hannink, *EMBO J.* **2006**, *25*, 3605.

[19] M. H. Tuszynski, L. Thal, M. Pay, D. P. Salmon, H. S. U, R. Bakay, P. Patel, A. Blesch, H. L. Vahlsing, G. Ho, G. Tong, S. G. Potkin, J. Fallon, L. Hansen, E. J. Mufson, J. H. Kordower, C. Gall, J. Conner, *Nat. Med.* **2005**, *11*, 551.

[20] a) X. Hu, X. Jing, *Expert Opin. Drug Delivery* **2009**, *6*, 1079; b) I. Ekladious, Y. L. Colson, M. W. Grinstaff, *Nat. Rev. Drug Discovery* **2019**, *18*, 273; c) Y. Zhang, Y. Lu, Y. Zhang, X. He, Q. Chen, L. Liu, X. Chen, C. Ruan, T. Sun, C. Jiang, *Mol. Pharmaceutics* **2017**, *14*, 3409.

[21] a) Z. Zhou, X. Ma, E. Jin, J. Tang, M. Sui, Y. Shen, E. A. Van Kirk, W. J. Murdoch, M. Radosz, *Biomaterials* **2013**, *34*, 5722; b) C. C. Lee, J. A. MacKay, J. M. Frechet, F. C. Szoka, *Nat. Biotechnol.* **2005**, *23*, 1517.

[22] V. Srikanth, A. Maczurek, T. Phan, M. Steele, B. Westcott, D. Juskiw, G. Munch, *Neurobiol. Aging* **2011**, *32*, 763.

[23] E. Gospodarska, A. Kupniewska-Kozak, G. Goch, M. Dadlez, *Biochim. Biophys. Acta.* **2011**, *1814*, 592.

[24] J. Li, H. Yang, Y. Zhang, X. Jiang, Y. Guo, S. An, H. Ma, X. He, C. Jiang, *ACS Appl. Mater. Interfaces* **2015**, *7*, 21589.

[25] J. Tan, Z. Deng, G. Liu, J. Hu, S. Liu, *Biomaterials* **2018**, *178*, 608.

[26] Y. Zhang, Q. Guo, S. An, Y. Lu, J. Li, X. He, L. Liu, Y. Zhang, T. Sun, C. Jiang, *ACS Appl. Mater. Interfaces* **2017**, *9*, 12227.

[27] M. Ma, N. Gao, X. Li, Z. Liu, Z. Pi, X. Du, J. Ren, X. Qu, *ACS Nano* **2020**, *14*, 9894.

[28] B. Kuhla, C. Loske, S. Garcia De Arriba, R. Schinzel, J. Huber, G. Munch, *J. Neural Transm.* **2004**, *111*, 427.

[29] R. Deane, S. Du Yan, R. K. Submamaryan, B. LaRue, S. Jovanovic, E. Hogg, D. Welch, L. Manness, C. Lin, J. Yu, H. Zhu, J. Ghiso, B. Frangione, A. Stern, A. M. Schmidt, D. L. Armstrong, B. Arnold, B. Liliensiek, P. Nawroth, F. Hofman, M. Kindy, D. Stern, B. Zlokovic, *Nat. Med.* **2003**, *9*, 907.

[30] I. Kratzer, K. Wernig, U. Panzenboeck, E. Bernhart, H. Reicher, R. Wronski, M. Windisch, A. Hammer, E. Malle, A. Zimmer, W. Sattler, *J. Controlled Release* **2007**, *117*, 301.

[31] Z. Cai, N. Liu, C. Wang, B. Qin, Y. Zhou, M. Xiao, L. Chang, L. J. Yan, B. Zhao, *Cell. Mol. Neurobiol.* **2016**, *36*, 483.

[32] Y. Kong, C. Liu, Y. Zhou, J. Qi, C. Zhang, B. Sun, J. Wang, Y. Guan, *Front. Aging Neurosci.* **2020**, *12*, 227.

[33] H. Xie, S. Hou, J. Jiang, M. Sekutowicz, J. Kelly, B. J. Bacskai, *Proc. Natl. Acad. Sci. USA* **2013**, *110*, 7904.

[34] C. M. Henstridge, B. T. Hyman, T. L. Spires-Jones, *Nat. Rev. Neurosci.* **2019**, *20*, 94.

[35] I. Buendia, P. Michalska, E. Navarro, I. Gameiro, J. Egea, R. Leon, *Pharmacol. Ther.* **2016**, *157*, 84.

[36] W. Zhang, C. Feng, H. Jiang, *Ageing Res. Rev.* **2021**, *65*, 101207.

[37] C. Madore, Z. Yin, J. Leibowitz, O. Butovsky, *Immunity* **2020**, *52*, 222.

[38] M. Colonna, O. Butovsky, *Annu. Rev. Immunol.* **2017**, *35*, 441.

[39] S. A. Wolf, H. W. Boddeke, H. Kettenmann, *Annu. Rev. Physiol.* **2017**, *79*, 619.

[40] T. Hamada, T. Aratake, Y. Higashi, Y. Ueba, T. Shimizu, S. Shimizu, T. Yawata, T. Ueba, R. Nakamura, T. Akizawa, M. Fujieda, M. Saito, *J. Trace Elem. Med. Biol.* **2020**, *61*, 126518.

[41] B. D. Arbo, L. R. Cechinel, R. P. Palazzo, I. R. Siqueira, *Ageing Res. Rev.* **2020**, *58*, 101006.

[42] M. T. Heneka, M. J. Carson, J. E. Khoury, G. E. Landreth, F. Brosseron, D. L. Feinstein, A. H. Jacobs, T. Wyss-Coray, J. Vitorica, R. M. Ransohoff, K. Herrup, S. A. Frautschy, B. Finsen, G. C. Brown, A. Verkhratsky, K. Yamanaka, J. Koistinaho, E. Latz, A. Halle, G. C. Petzold, T. Town, D. Morgan, M. L. Shinohara, V. H. Perry, C. Holmes, N. G. Bazan, D. J. Brooks, S. Hunot, B. Joseph, N. Deigendesch, O. Garaschuk, E. Boddeke, C. A. Dinarello, J. C. Breitner, G. M. Cole, D. T. Golenbock, M. P. Kummer, *Lancet Neurol.* **2015**, *14*, 388.

[43] H. Yang, X. Li, L. Zhu, X. Wu, S. Zhang, F. Huang, X. Feng, L. Shi, *Adv. Sci.* **2019**, *6*, 1901844.

[44] R. Liu, J. Yang, L. Liu, Z. Lu, Z. Shi, W. Ji, J. Shen, X. Zhang, *Adv. Sci.* **2020**, *7*, 1901555.

[45] K. L. Viola, W. L. Klein, *Acta Neuropathol.* **2015**, *129*, 183.

[46] I. López-González, A. Schlüter, E. Aso, P. Garcia-Esparcia, B. Ansoleaga, L. L. Franc, M. Carmona, J. Moreno, A. Fuso, M. Portero-Otin, R. Pamplona, A. Pujol, I. Ferrer, *J. Neuropathol. Exp. Neurol.* **2015**, *74*, 319.

[47] D. W. Wesson, D. A. Wilson, *Behav. Brain Res.* **2011**, *216*, 408.

[48] P. Poprac, K. Jomova, M. Simunkova, V. Kollar, C. J. Rhodes, M. Valko, *Trends Pharmacol. Sci.* **2017**, *38*, 592.

[49] E. A. Bordt, B. M. Polster, F. Radic, *Biol. Med.* **2014**, *76*, 34.

[50] S. Kartha, C. L. Weisshaar, R. A. Pietrofesa, M. Christofidou-Solomidou, B. A. Winkelstein, *Antioxidants* **2020**, *9*, 1209.

[51] A. Nunomura, G. Perry, G. Aliev, K. Hirai, A. Takeda, E. K. Balraj, P. K. Jones, H. Ghanbari, T. Wataya, S. Shimohama, S. Chiba, C. S. Atwood, R. B. Petersen, M. A. Smith, *J. Neuropathol. Exp. Neurol.* **2001**, *60*, 759.

[52] S. M. Ahmed, L. Luo, A. Namani, X. J. Wang, X. Tang, *Biochim. Biophys. Acta, Mol. Basis. Dis.* **2017**, *1863*, 585.

[53] R. M. Ransohoff, *Science* **2016**, *353*, 777.

[54] A. M. Arranz, B. De Strooper, *Lancet Neurol.* **2019**, *18*, 406.

[55] A. Adachi, F. Kano, T. C. Saido, M. Murata, *Genes Cells* **2009**, *14*, 355.

[56] M. A. Mobasher, A. Gonzalez-Rodriguez, B. Santamaria, S. Ramos, M. A. Martin, L. Goya, P. Rada, L. Letzig, L. P. James, A. Cuadrado, J. Martin-Perez, K. J. Simpson, J. Muntane, A. M. Valverde, *Cell Death Dis.* **2013**, *4*, e626.